



Orientation of H platelets under local stress in Si

S. Reboh, M. F. Beaufort, J. F. Barbot, J. Grilhé, and P. F. P. Fichtner

Citation: *Applied Physics Letters* **93**, 022106 (2008); doi: 10.1063/1.2958212

View online: <http://dx.doi.org/10.1063/1.2958212>

View Table of Contents: <http://scitation.aip.org/content/aip/journal/apl/93/2?ver=pdfcov>

Published by the [AIP Publishing](#)



Re-register for Table of Content Alerts

Create a profile.



Sign up today!



Orientation of H platelets under local stress in Si

S. Reboh,^{1,2} M. F. Beaufort,² J. F. Barbot,^{2,a)} J. Grilhé,² and P. F. P. Fichtner¹

¹Escola de Engenharia, Universidade Federal do Rio Grande do Sul, Porto Alegre 91501-970, Brazil

²Laboratoire de Physique des Matériaux, UMR6630, Université de Poitiers, 86962 Futuroscope, France

(Received 26 May 2008; accepted 21 June 2008; published online 16 July 2008)

Hydrogen is implanted into (001) silicon under the strain field of previously formed overpressurized helium plates. Upon thermal annealing, the hydrogen atoms precipitate into platelet structures oriented within specific {111} or {001} variant determined through the local symmetry of the strain. The behavior is understood in terms of elastic interactions and is described via energy minimization calculations, predicting the formation and distribution of each platelet orientation variant. Our results demonstrate the concept that sublocal organized arrangements of precipitates can be obtained within nanosize domains using local strain fields. © 2008 American Institute of Physics.

[DOI: 10.1063/1.2958212]

Hydrogen in Si is known to precipitate in two-dimensional (2D) cavities named H-platelets, which preferentially form parallel to the surface when H is introduced via ion implantation. Their evolution under annealing has been studied in detail (for a review of hydrogen blistering in Si, see Ref. 1). In contrast, by plasma hydrogenation, the platelets lie onto the {111} planes. This difference is related to the in-plane stress induced by the implantation technique.² Strain can drive preferential nucleation of platelet variants.^{3,4} In the present contribution, we demonstrate the possibility of exploiting local strain sources to tailor a sublocal architecture of H platelets, creating organized nanodomains. In particular, we use overpressurized helium filled platelike structures produced by helium implantation in (001) Si substrates,⁵ which act as the local strain sources patterning a symmetrical arrangement of platelets produced by hydrogen postimplantation. The observations are well described by model calculations based on elastic interactions and formation energies of platelets. We also propose that nanoscale strain engineering can further be developed and generalized as a tool to tailor specific arrangements of nanoprecipitates discrete nanodomains of a periodic array. The organization of such nanoprecipitates within particular orientations, concentrations, and symmetries at the nanometer scale allows the emergence of collective excitation modes.⁶⁻⁸

The experiments were performed using 1–20 Ω cm p-type (001) Si. The samples were submitted to two steps of implantation, each one followed by annealing. In the first step, He⁺ ions were implanted at 45 keV at a fluence of $1 \times 10^{16} \text{ cm}^{-2}$, and the samples were annealed at 350 °C for 900 s in high vacuum. Overpressurized platelike cavities² (He plates) oriented parallel to the surface are expected to form at a depth close to the mean projected range of the He ions ($R_p^{\text{He}} \approx 385 \text{ nm}$ according to the stopping and range of ions in matter (SRIM) calculations⁹). In the second step, the samples were implanted with 30 keV H₂⁺ ions at $0.5 \times 10^{16} \text{ cm}^{-2}$ and annealed at 300 °C for 1800 s, leading to the precipitation of H platelets at $\approx 200 \text{ nm}$ from the strain sources (i.e., the He plates). The implantations were performed at room temperature with a current density of $0.5 \mu\text{A cm}^{-2}$. The specimens were characterized by trans-

mission electron microscopy (TEM) in cross-sectional samples and observed at 200 keV in a JEM 2010 microscope.

The first implantation/annealing step forms He plates lying on the (001) habit planes parallel to the surface at a depth $\approx R_p^{\text{He}}$. The second implantation/annealing step produces an H related damaged region located between the He related damage layer and the surface. Figure 1 shows the resulting microstructure. In the zones where He plates were not present directly underneath, the H platelets are found to be preferentially aligned parallel along the (001) planes. For regions directly above a He plate, the H platelets are preferentially aligned to specific {111} lattice variants with respect to the strain field symmetry axis [001]. The orientation of H platelets is clearly influenced by the local strain field of the He plate. Due to its cylindrical symmetry, the four possible {111} variants of H platelets are arranged in a quadrant architecture. Two {111} variants are observed when imaging along the [-110] direction (Fig. 1); the two other being seen when performing the observations along the [-1-10] direction. The pictographs in Fig. 2 illustrate the three dimensional (3D) representation of the nanostructure. The normal direction of each platelet variant group converges into the [001] axis. This is an example of unique nanoscale geometrical arrangement of objects with a local fourfold rotation symmetry.

A model based on elastic interactions for the nucleation of H-precipitates in a semi-infinite solid was then developed. To simplify, the calculation was conducted in 2D, the He plate was modeled as an edge dislocation dipole running along the y axis, i.e., the [-1-10] direction of the crystal, and the H-precipitates were modeled as dislocation loops¹⁰ of interstitial nature (Burgers vector $\vec{b} = -b\vec{n}$).

The energy of formation E^T of H platelets under the influence of a strain field is given by

$$E^T = E_f + \int \vec{b}_H \cdot \Sigma \cdot d\vec{S}, \quad (1)$$

where E_f is the self-energy, $d\vec{S} = dS \cdot \vec{n}$ a surface element, and Σ is a total stress tensor caused by both the overpressurized He plate and the implantation (in-plane stress). The components of the elastic stress field were then obtained by solving the appropriate Airy's stress function.¹¹ However, due to the

a) Author to whom corresponding should be addressed. Electronic mail: jean.francois.barbot@univ-poitiers.fr.

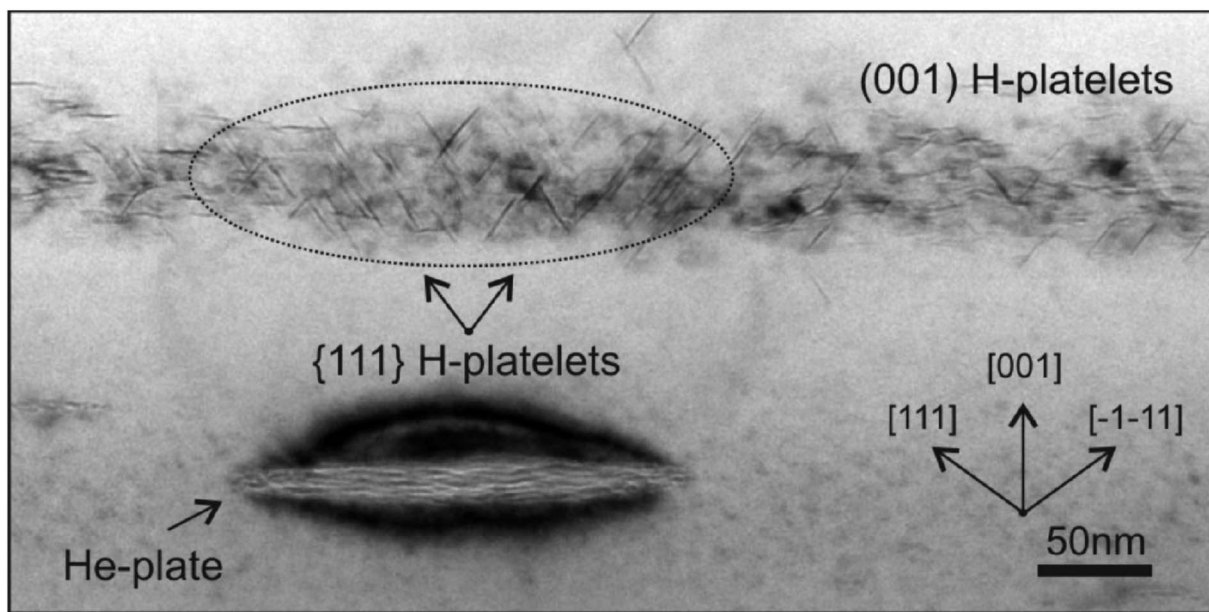


FIG. 1. Bright-field TEM image, kinematical diffraction condition, overfocus, taken after the He-plate formation, followed by H_2^+ implantation (30 keV , $5 \times 10^{15} \text{ cm}^{-2}$ and annealing at $300 \text{ }^\circ\text{C}$ for 1800 s). A specific arrangement of $\{111\}$ H platelets is observed where the He-plate is located underneath. Beyond the H platelets are found lying on the (001) planes parallel to the surface.

proximity of a free surface, a second dipole of image dislocations with opposite Burgers vector at the mirror position outside the crystal as well a surface distribution of Boussinesq's forces were also introduced. The in-plane stress due to the implantation is given by $\sigma_{yy}^{\text{in-plane}} = -2\mu(\partial d/d)_z$, where $(\partial d/d)_z$ is the z -dilatation of the lattice due to the H-implantation. This dilatation was taken as constant at its maximum value, allowing a description of the H platelet variant distribution to any chosen R_p^H . The energy density variation ΔE of the platelets is then

$$\Delta E = -(n_y^2 \sigma_{yy}^* + 2n_y n_z \sigma_{zy}^* + n_z^2 \sigma_{zz}^*), \quad (2)$$

where (n_y, n_z) values are the projections in 2D of the unit Burgers vectors to each variant, i.e., $(0,1)$ and $(-\sqrt{2}/\sqrt{3}, 1/\sqrt{3})$ for the (001) and (111) H platelets, respectively. Their formation energy E_f was assumed to be similar¹² even if TEM observations suggest that $E_f^{(100)} > E_f^{(111)}$; it does not affect the results much. Finally, the calculations were done by introducing a factor k , which is defined as¹³

$$k = a \frac{4\pi(1-\nu)}{b_{\text{eff}}^{\text{He plate}}} \left(\frac{\partial d}{d} \right)_z, \quad (3)$$

where μ is the shear modulus, ν is the Poisson's ratio, a is the radius of the He plate, and $b_{\text{eff}}^{\text{He plate}}$ is the effective Burgers vector of the He plate. The effective Burgers vector $b_{\text{eff}}^{\text{He plate}} \approx 7 \text{ nm}$ was estimated from the calculations of $\sigma_{zz}(0, R_p^{\text{He}})$ and assuming a He plate with a radius $a = 100 \text{ nm}$ under thermal equilibrium pressure conditions.¹⁴ The maximum of the strain for $0.5 \times 10^{16} \text{ cm}^{-2} H_2^+$ was estimated to be on the order of 0.3%.¹⁵ This leads to a value of $k=0.4$.

Figure 3 is a map of isoenergetic regions plotted with ΔE intervals of 0.1 ($\approx 100 \text{ MPa}$); the calculations were done using a unit of length $a=100 \text{ nm}$. Whereas the isoenergetic regions for the (001) platelets [Fig. 3(b)] are symmetrically distributed around the stress symmetry axis z , the (111)

platelet map [Fig. 3(a)] presents asymmetry where the particular (111) variant is favorable (i.e., has the lowest E^T) in one quadrant of the 3D structure. Figure 3(c) shows the ΔE level variations at the depth $z=R_p^{\text{He}}/2 \approx R_p^H$. The formation of the (111) platelets is favorable from $y=0$ up to $y \approx 1.5a$, in good agreement with the TEM observations (see Fig. 1).

By changing the conditions of H-implantation, different distributions of the (111) and (001) platelets can be pre-

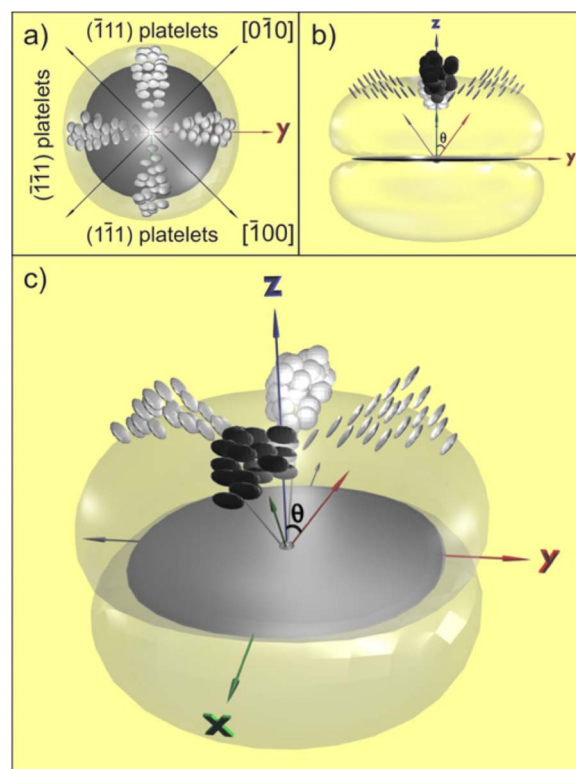


FIG. 2. (Color online) 3D pictograph of the nanostructure: (a) top view with the four $\{111\}$ variants of the H platelets in their respective quadrant, (b) front view, and (c) perspective view.

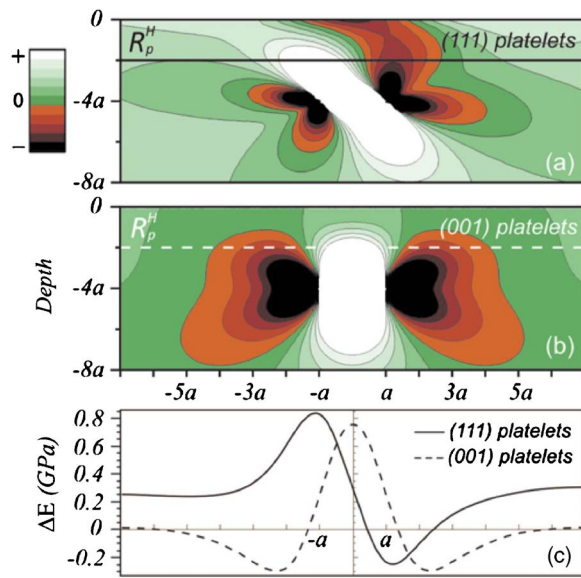


FIG. 3. (Color online) Maps of isoenergy regions of (a) (111) platelets and (b) (001) platelets. The curves in (c) show the ΔE level variations at $z = -2a$ for (111) platelets (continuous line) and (001) platelets (dashed line).

dicted. Moreover, Eq. (1) suggests that even a precipitate with higher self-energy ($E_{f1} > E_{f2}$) could be favored by an appropriate stress tensor, resulting in $E_1^T < E_2^T$. In this way, one could imagine that by adequate stress engineering, it is possible to induce the appearance of precipitates that have not already been observed due to their unfavorable self-energy.

In conclusion, we demonstrate that in (001) silicon, four specific {111} variants of H platelets can be exclusively formed within an auto-organized nanometer domain determined by the symmetry axis of a local strain field. The phe-

nomenon has been modeled and the results are in good agreement with the experimental observations. Other geometries of strain fields will certainly conduct different arrangements of precipitates. Hence, these results set the basis for the formation of localized and controlled 3D arrangements of objects at the nanoscale level using a bottom-up local strain-engineering approach.

The authors would like to thank the CAPES COFECUB program for financial support. S. Reboh is also indebted to the French ambassador in Brasil and the ‘‘SPI&A Ecole doctorale’’ for their financial participation.

¹B. Terreault, *Phys. Status Solidi A* **204**, 2129 (2007).

²A. J. Pitera and E. A. Fitzgerald, *J. Appl. Phys.* **97**, 104511 (2005).

³X. Hebras, P. Nguyen, K. K. Bourdelle, F. Letertre, N. Cherkashin, and A. Claverie, *Nucl. Instrum. Methods Phys. Res. B* **262**, 24 (2007).

⁴M. Nastasi, T. Höchbauer, J. K. Lee, A. Misra, J. P. Hirth, M. Ridgway, and T. Lafford, *Appl. Phys. Lett.* **86**, 154102 (2005).

⁵P. F. P. Fichtner, J. R. Kaschny, R. A. Yankov, A. Mücklich, U. Kreißig, and W. Skorupa, *Appl. Phys. Lett.* **70**, 732 (1997).

⁶H. A. Atwater, S. Maier, A. Polman, J. A. Dionne, and L. Sweatlock, *MRS Bull.* **30**, 385 (2005).

⁷J. S. Biteen, L. A. Sweatlock, H. Mertens, N. S. Lewis, A. Polman, and H. A. Atwater, *J. Phys. Chem. C* **111**, 13372 (2007).

⁸T. T. Kang, R. Q. Zhang, W. G. Hu, G. W. Cong, F. A. Zhao, X. X. Han, S. Y. Yang, X. L. Liu, Q. S. Zhu, and Z. G. Wang, *Phys. Rev. B* **76**, 075345 (2007).

⁹J. F. Ziegler, and J. B. Biersack, <http://www.srim.org>.

¹⁰J. Grisolia, Ph.D. thesis, France, 2000.

¹¹J. P. Hirth and J. Lothe, *Theory of Dislocations* (Wiley, New York, 1982).

¹²N. Martsinovich, I. S. Martínez, and M. I. Heggie, *Phys. Status Solidi C* **2**, 1771 (2005).

¹³The factor k , which characterizes the intensity of the in-plane stress, has been defined as $k = \sigma_{yy}^{\text{in-plane}}/D$, where D is the prefactor of the Airy’s function of an edge dislocation.

¹⁴M. Hartmann and H. Trinkaus, *Phys. Rev. Lett.* **88**, 055505 (2002).

¹⁵D. Bisero, F. Corni, S. Frabboni, R. Tonini, G. Ottaviani, and R. Balboni, *J. Appl. Phys.* **83**, 4106 (1998).